Revista Colombiana de Estadística
July 2016, Volume 39, Issue 2, pp. 185 to 204
DOI: http://dx.doi.org/10.15446/rce.v39n2.58915

A Study of Cumulative Quantity Control Chart for a Mixture of Rayleigh Model under a Bayesian Framework

Un estudio de cartas de control de cantidades acumuladas por mixturas de modelos Rayleigh bajo un enfoque Bayesiano

Tabassum Naz Sindhu[1,a], Muhammad Riaz[2,b], Muhammad Aslam[3,c], Zaheer Ahmed[4,d]

[1]Department of Statistics, Quaid-i-Azam University, Islamabad, Pakistan

[2]Department of Mathematics and Statistics, King Fahad University of Petroleum and Minerals, Dhahran, Saudi Arabia

[3]Department of Basic Sciences, Riphah International University, Islamabad, Pakistan

[4]Department of Applied Mathematics and Statistics, Institute of Space Technology, Islamabad, Pakistan

Abstract

This study deals with the cumulative charting technique based on a simple and a mixture of Rayleigh models. The respective charting schemes are referred as the SRCQC-chart and the MRCQC-chart. These are stimulated from existing statistical control charts in this direction i.e. the cumulative quantity control (CQC) chart, based on exponential and Weibull models, and the cumulative count control (CCC) chart, based on the simple geometric model. Another motivation for this study is the mixture cumulative count control (MCCC) chart based on the two component geometric model. The use of mixture cumulative quantity is an attractive approach for process monitoring. The design structure of the proposed control chart is derived by using the cumulative distribution function of simple, and two components of mixture distribution(s). We observed that the proposed charting structure is efficient in detecting the changes in process parameters. The application of the proposed scheme is illustrated using a real dataset.

***Key words*:** Quality control, Inverse transformation method, Loss functions and bayes estimators, MRCQC-Chart, SRCQC-Char.

[a]Professor. E-mail: sindhuqau@gmail.com
[b]Professor. E-mail: riaz76qau@yahoo.com
[c]Professor. E-mail: aslamsdqu@yahoo.com
[d]Professor. E-mail: zaheerqau77@gmail.com

Resumen

Este estudio trata con cartas de control acumuladas basadas en distribuciones Rayleigh y en mixturas de estas mismas. Las cartas se denominan SRCQC y MRCQC, respectivamente. Estas se fundamentan en cartas existentes como la carta de control de cantidades acumuladas (CQC), basada en modelos exponencial y Weibull en la carta de control de conteos acumulados (CCC), soportada en un modelo geométrico. Otra propuesta del estudio es la carta de control de mixtura de conteos acumulados (MCCC). Esta última es muy atractiva en procesos de monitoreo. La estructura de diseño de las cartas propuestas se deriva usando la función de distribución acumulada simple y la mixtura de dos distribuciones acumuladas. Se observa que las cartas propuestas son eficientes para detectar cambios en los parámetros del proceso. La aplicación del esquema propuesto es ilustrada usando un conjunto de datos reales.

***Palabras clave*:** control de calidad, método de la transformación, función de pérdida, estimador bayesiano, carta MRCQC, carta SRCQC.

1. Introduction

Mixture distributions are quite popular when modelling populations containing two or more subgroups. These probability models represent non-homogenous behavoiurs and may be utilized in manufacturing and non-manufacturing applications for the characteristic(s) of interest that exhibit mixture patterns. These types of mixtures offer a more valuable analysis that leads to more meaningful results. It is important to properly model the variable of interest by using simple or mixture models and to estimate their parameters with the assistance of accessible information. The estimation of parameters may be carried out using classical and Bayesian methods of estimation.

Control charts are popular process monitoring tools that may be categorized mainly into variable and attribute control charts. The most commonly used attribute charts are p chart or np chart (binomial data), and the c charts or u chart (Poisson data). These two types of traditional attribute charts have been replaced by other types of charts such as the cumulative count control chart (CCC-chart) and the cumulative quantity control charts (CQC-chart). These charts are much more effective than the traditional charts for high yield processes when the nonconforming rate is low. In addition, these types of charts require no rational sub grouping of samples, and the issue of increased false alarm may be avoided. Please see Calvin (1983), Xie & Goh (1992), Xie, Goh & Kuralmani (2000) and Xie, Goh & Tang (2000). The cumulative types CCC and CQC charts use geometric and exponential models. We can also find the application of other probability distributions with these types of charts such as weibull (cf. Chan, Xie & Goh 2000, Banjevic, Jardine, Makis & Ennis 2001, Sun, Yang, del Rosario & Murphy 2001 and Xie, Goh & Ranjan 2002). Chan, Lin, Xie & Goh (2002) designed the cumulative probability control charts for geometric and exponential process characteristic(s). Majeed, Aslam & Riaz (2012) suggests that mixture cumulative

count control charts be used for mixture geometric process characteristics, when a population of defective items can be split into various sub populations.

There are varying dimensions to be considered when developing different types of charts for time between events situations. Different statistical models are used to model processes with constant or variable occurrence rate of event. The time-between events data is generally modeled by an exponential distribution, assuming that the event occurrence rate is constant. In reliability applications this assumption is usually violated because of wear and tear and other usage factors. In such situations, Rayleigh distribution (in simple or mixture form depending upon the situation) may be a more appropriate choice to model the failure times. This study enlightens the Bayesian estimation of the mixture Rayleigh model(s) and proposes a new control, chart namely the mixture of cumulative quantity control chart for Rayleigh process characteristic(s) (MRCQC-chart). It is designed by using the distribution function of two component Rayleigh model. The case of the simple Rayleigh cumulative quantity control chart (SRCQC-chart) is also dicussed throng along the paper.

The rest of the article is organized as follows: Section 2 provides details of mixture Rayleigh distribution and its Bayesian estimation; Section 3 shows the development of a new of mixture charting structures and its performance and methodology evaluation; Section 4 presents an applied example; Section 5 concludes the study.

2. Mixture Rayleigh Model and Bayes Estimation

Rayleigh is a commonly used distribution to analyze lifetime data; it has attractive properties and nice physical interpretations. In this study we use it in a mixture setup for process monitoring purposes. Let us suppose that a population of nonconformities is postulated to be composed of two subpopulations with specified parameters. The fractions of nonconformities produced by Poisson process from both sub-populations are denoted by λ_1 and λ_2, respectively. The subpopulations are mixed are have the proportions p_1 and p_2. In this is situation happening, the total quantity Q' examined until an event of interest occurs (with a non-constant event occurrence rate) and follows a two component mixture of Rayleigh distribution. The following a finite mixture distribution function with the two component densities of specified parametric form (but with unknown rate parameters, λ_1 and λ_2) and with unknown mixing weights, p_1 and p_2:

$$F(q) = p_1 F_1(q) + p_2 F_2(q), \quad \text{where} \quad F_i(q_{ij}) = 1 - \exp\left[-q_{ij}^2 \lambda_i^2\right]. \tag{1}$$

The corresponding finite mixture density function's pdf is:

$$f(q_{ij}; \Theta) = p_1 f_1(q_{1j}; \lambda_1) + p_2 f_2(q_{2j}; \lambda_2), \ \lambda_i > 0, \ i = 1, 2; \ 0 < q_{ij} < \infty, \tag{2}$$

where $\Theta = (\lambda_1, \lambda_2, p_1)$, $f_i(q_{ij}) = 2q_{ij}\lambda_i^2 \exp\left[-\lambda_i^2 q_{ij}^2\right]$, $j = 1, 2, \ldots, r_i$ and $p_1 + p_2 = 1$.

A random sample of n units of quantity from the above cited mixture model is operating to a life testing experiment. The test is terminated at a fixed time Q. When the the test is performed, it is observed that out of n, r units of quantity failed when the test termination time Q and $(n-r)$ units when still functioning (conformities). Hence $(n-r)$ units of quantity that have not failed (conformities) by the time Q are censored objects and yield no information. We suppose that, soon after, failure occurs, we can identify r_1 and r_2 units of quantity as members of the first and second subpopulation, respectively. Obviously $r = r_1 + r_2$ and remaining $(n-r)$ units provide no information about to which they belong. Furthermore, let q_{ij} be the failure time of the j^{th} unit to the i^{th} subpopulation, where $j = 1, 2, \ldots, r_i$, $i = 1, 2$ $0 < q_{1j}, q_{2j} < Q$. This sampling plan was introduced by Mendenhall & Hadar (1958). The likelihood function for a two-component mixture with n items is the obtained of this study. The probability that r_1 will fail due to cause 1, r_2 will fail due to cause 2 and the remaining $(n - r_1 - r_2)$ will survive at time Q when test is terminated is given as

$$L(\Theta \mid q) \propto \Pi_{j=1}^{r_1} p_1 f_1(q_{1j}) \Pi_{j=1}^{r_2} p_2 f_2(q_{2j}) \{1 - F(Q)\}^{n-r},$$

$$L(\Theta \mid q) \propto \left\{\Pi_{j=1}^{r_1} p_1 2 q_{1j} \lambda_1^2 \exp\left(-\lambda_1^2 q_{1j}^2\right)\right\} \left\{\Pi_{j=1}^{r_2} p_2 2 q_{2j} \lambda_2^2 \exp\left(-\lambda_2^2 q_{2j}^2\right)\right\} \left[1 - \left\{p_1\left(1 - \exp\left(-\lambda_1^2 Q^2\right)\right) + p_2 \exp\left(1 - \exp\left(-\lambda_2^2 Q^2\right)\right)\right\}\right]^{n-r},$$

$$L(\Theta \mid q) \propto \sum_{k=0}^{n-r} \binom{n-r}{k} p_1^{n-k-r_2} p_2^{r_2+k} \lambda_1^{2r_1} \lambda_2^{2r_2} \exp\left[-\lambda_1^2 \left(\xi_{1j}(q_{1j})\right)\right] \times \exp\left[-\lambda_2^2 \left(\xi_{2j}(q_{2j})\right)\right], \quad (3)$$

where $\xi_{1j}(q_{1j}) = \sum_{j=1}^{r_1} q_{1j}^2 + (n-r-k) Q^2$ and $\xi_{2j}(q_{2j}) = \sum_{j=1}^{r_2} q_{2j}^2 + kQ^2$.

The parameters of mixture model $\Theta = (\lambda_1, \lambda_2, p_1)$ can be estimated by using different methods. In this article, we utilize a Bayesian approach in order to obtain the estimators of the mixture model. The elegant closed-form expressions of Bayes estimates and their risks are proposed in following section.

2.1. Bayes Estimation

Bayesian estimation theory requires independent priors to be specified for a model's parameters. The prior model is assumed to represent the subjective information available concerning the parameter vector prior to the realization of the sample vector. Let us assume that the rate parameters λ_i and p_1 $i = 1, 2$ are independent random variables. We can consider that the following informative priors for different parameters provide the Bayes estimates.

2.2. Bayesian Estimation using Nakagami Prior

The prior for the rate parameters λ_i for $i = 1, 2$, is the Nakagami distribution. The hyperparameters a_i and b_i are given by:

$$f_{\lambda_i}(\lambda_i) = \frac{2a_i^{a_i}}{\Gamma(a_i)\, b_i^{a_i}} \lambda_i^{2a_i-1} \exp\left(\frac{-a_i\lambda_i^2}{b_i}\right), \quad a_i, b_i > 0. \tag{4}$$

The prior for p_1 is the beta distribution, the density of which is given by

$$f_p(p_1) = \frac{\Gamma(c_1+d_1)}{\Gamma(c_1)\,\Gamma(d_1)} p_1^{c_1-1}(1-p_1)^{d_1-1}, \quad c_1, d_1 > 0. \tag{5}$$

Based of equation (4)-(5), we recommend the following joint prior density of the vector $\Theta = (\lambda_1, \lambda_2, p_1)$

$$g(\Theta) \propto \lambda_i^{2a_i-1} \exp\left(\frac{-\lambda_i^2 a_i}{b_i}\right) p_1^{c_1-1}(1-p_1)^{d_1-1}, \tag{6}$$

where $0 < p_1 < 1$, $a_i > 0$, $b_i > 0$, $c_1 > 0$, $d_1 > 1$.

By multiplying equation (6) with equation (3), the joint posterior density for the vector Θ given the data becomes

$$L(\Theta \mid q) \propto \sum_{k=0}^{n-r} \binom{n-r}{k} p_1^{n-k-r_2+c_1-1}(1-p_1)^{r_2+k+d_1-1} \lambda_i^{2(a_i+r_i)-1} \times \exp\left\{-\lambda_i^2\left(\frac{a_i}{b_i} + \xi_{ij}(q_{ij})\right)\right\}. \tag{7}$$

Marginal distributions of λ_i and p_1 $i = 1, 2$ can be obtained by integrating the nuisance parameters.

2.3. Bayesian Estimation Using Square Root Gamma Prior

The prior for the rate parameters λ_i for $i = 1, 2$ is the square root gamma distribution. The hyperparameters α_i and β_i, given by:

$$f_{\lambda_i}(\lambda_i) = \frac{2\beta_i^{\alpha_i}}{\Gamma(\alpha_i)} \lambda_i^{2\alpha_i-1} \exp\left(-\lambda_i^2\beta_i\right), \quad \alpha_i, \beta_i > 0. \tag{8}$$

The prior for p_1 is the beta distribution, the density of which is given by

$$f_p(p_1) = \frac{\Gamma(c_2+d_2)}{\Gamma(c_2)\,\Gamma(d_2)} p_1^{c_2-1}(1-p_1)^{d_2-1}, \quad c_2, d_2 > 0. \tag{9}$$

Based of equation (8)-(9), we present the following joint prior density of the vector $\Theta = (\lambda_1, \lambda_2, p_1)$

$$g(\Theta) \propto \lambda_i^{2\alpha_i-1} \exp\left(-\lambda_i^2\beta_i\right) p_1^{c_2-1}(1-p_1)^{d_2-1}, \tag{10}$$

where $0 < p_1 < 1$, $\alpha_i > 0$, $\beta_i > 0$,$c_2 > 0$, $d_2 > 0$.

By multiplying equation (10) with equation (3), the joint posterior density for the vector Θ given the data becomes

$$L(\Theta \mid q) \propto \sum_{k=0}^{n-r} \binom{n-r}{k} p_1^{n-k-r_2+c_2-1} (1-p_1)^{r_2+k+d_2-1} \lambda_i^{2(\alpha_i+r_i)-1} \times \exp\left\{-\lambda_i^2 (\beta_i + \xi_{ij}(q_{ij}))\right\}. \quad (11)$$

Marginal distributions λ_i and p_1 $i = 1, 2$ of can be obtained by integrating the nuisance parameters.

2.4. Bayes Estimation of the Vector of Parameters Θ

The Bayesian point estimation is generally associated with a loss function. It adds up the loss induced when the estimate $\hat{\lambda}$ deviates from true parameter λ. In this article, have used weighted balanced loss function (WBLF) and precautionary loss function (PLF). The WBLF is particularized as $l\left(\hat{\theta}, \theta\right) = \left[\frac{(\theta-\hat{\theta})}{\hat{\theta}}\right]^2$, Degroot (1970). Bayes estimator and posterior risk under WBLF are $\hat{\theta} = \frac{E(\theta^2|q)}{E(\theta|q)}$, and $\rho\left(\hat{\theta}\right) = 1 - \frac{\{E(\theta|q)\}^2}{E(\theta^2|q)}$. The other loss function PLF is defined as $l\left(\hat{\theta}, \theta\right) = \frac{(\theta-\hat{\theta})^2}{\hat{\theta}}$, Norstrom (1996). Bayes estimator and posterior risk under PLF are $\hat{\theta} = \left[E\left(\theta^2 \mid q\right)\right]^{1/2}$ and $\rho\left(\hat{\theta}\right) = 2\left[\left\{E\left(\theta^2 \mid q\right)\right\}^{1/2} - E\left(\theta \mid q\right)\right]$ respectively.

In this section, the respective marginal distribution of each parameter is used to derive the Bayes estimators and posterior risks of λ_1, λ_2 and p_1 under different loss functions. The Bayes estimators and their posterior risks of the parameters λ_1, λ_2 and p_1 using Nakagamiandbeta under WBLF are given in Appendix:

The expressions for the Bayes estimators and their posterior risks under PLF and the Bayes estimators, and their posterior risks using square root prior under two loss functions can be obtained in similar ways.

The Bayes estimators and their post risks are derived from a simple Rayleigh model (SRM) using Nakagami distribution under both loss functions. These are given in Aappendix:

2.5. Elicitation of Hyperparameters

In Bayesian estimation, the elicitation of hyperparameters plays a consequential role and hence their estimation is additionally concerned. We consider a probability elicitation method: prior predictive elicitation. Predictive elicitation is a method used to estimate hyperparameters of prior distributions. Elicitation of hyperparameters from the prior $p(\lambda)$ is a conceptually arduous task because we first have to identify prior distribution and then its hyperparameters. The prior predictive distribution is utilized to elicit of the hyperparameters which a compared

to the experts' judgment about this distribution. after this, the hyperparameters are culled in such a way so as to make the judgment to be close as possible to the given distribution (cf. Grimshaw, Collings, Larsen & Hurt 2001, O'Hagan, Buck, Daneshkhah, Eiser, Garthwaite, Jenkinson, Oakley & Rakow 2006, Jenkinson and Leon, Vazquez-Polo & Gonzalez).

According to Aslam (2003), the assessment method is to compare the predictive distribution with experts' assessments on this distribution and then to operate the hyperparameters that make the assessment accede proximately with the member of the family. The hyperparameters involved in the evaluation of Bayes estimates and Posterior risks have been elicited yb applying the prior predictive approach; the prior predictive distribution under all the priors are derived by using the following formula $p(y) = \int_{\Theta} p(y \mid \Theta)\, p(\Theta)\, d\Theta$. The prior predictive distribution using Nakagami prior is:

$$\begin{aligned} p(y) = 2\left(\frac{a_1}{b_1}\right)^{a_1} & \frac{y a_1 c_1}{(c_1+d_1)\left(y^2+\frac{a_1}{b_1}\right)^{(a_1+1)}} \\ + 2\left(\frac{a_2}{b_2}\right)^{a_2} & \frac{y a_2 d_1}{(c_1+d_1)\left(y^2+\frac{a_2}{b_2}\right)^{(a_2+1)}}, \quad y>0. \end{aligned} \tag{12}$$

To the six hyperparameters, six different intervals are considered. From equation (12), the experts' assessments are supposed to be $0.15, 0.10, 0.10, 0.10, 0.15$ and 0.20; which are related to the intervals of the values of the random variable Y: $(0,5)$, $(6,9)$, $(7,10)$, $(20,23)$, $(30,35)$ and $(30,40)$ respectively. For elicitation of six hyperparameters a_1, a_2, b_1, b_2, c_1, and d_1. These six equations are solved simultaneously through a computer program developed in SAS package using the PROC SYSLIN command. Thus the values of hyperparameters obtained by applying this methodology are 0.45231, 0.012109, 0.52114, 4.99325, 2.52130, and 1.6259.

The prior predictive distribution using square root gamma prior is:

$$\begin{aligned} p(y) = 2\left(\beta_1\right)^{\alpha_1} & \frac{y \alpha_1 c_1}{(c_2+d_2)\left(y^2+\beta_1\right)^{(\alpha_1+1)}} \\ + 2\left(\beta_2\right)^{\alpha_2} & \frac{y \alpha_2 d_2}{(c_2+d_2)\left(y^2+\beta_2\right)^{(\alpha_2+1)}}, \quad y>0. \end{aligned} \tag{13}$$

By applying the similar principle that was defined for the Nakagami prior, we obtained the following values of hyperparameters: $\alpha_1 = 1.32156$, $\alpha_2 = 0.96856$, $\beta_1 = 0.52114$, $\beta_2 = 2.36916$, $c_2 = 1.25698$ and $d_2 = 0.96845$.

The simulation study for the Bayes estimators (BEs) and their corresponding posterior risks are given under different priors for the mixture (cf. Table 1) and simple (cf. Table 2) models. We have observed that the Bayes estimators under Nakagami are more efficient and have a clear edge are its competitor informative prior fort he mixture as well as simple models.

TABLE 1: Bayes estimates (and their posterior risks in parentheses) for parametric points $(\lambda_1, \lambda_2, p_1) = (0.1, 0.15, 0.45)$. Bayes estimates (and their posterior risks in parentheses) for parametric point $\lambda = 0.15$.

LF	WBLF			PLF		
Priors	$\hat{\lambda}_1$	$\hat{\lambda}_2$	$\hat{p}_1$	$\hat{\lambda}_1$	$\hat{\lambda}_2$	$\hat{p}_1$
Nakagami	0.103179	0.149154	0.447361	0.102746	0.148945	0.444672
	(0.005957)	(0.004839	(0.007797)	(0.000628)	(0.000713)	(0.003453)
Square root	0.104053	0.149865	0.444932	0.103538	0.149374	0.44924
gamma	(0.006131)	(0.004921)	(0.008114)	(0.000646)	(0.000726)	(0.003557)

TABLE 2: Bayes estimates (and their posterior risks in parentheses) for parametric point $\lambda = 0.15$.

LF	WBLF	PLF
Priors	$\hat{\lambda}$	$\hat{\lambda}$
Nakagami	0.152801	0.152497
	(0.000805)	(0.000123)
Square root gamma	0.151678	0.149865
	(0.000818)	(0.000124)

3. Control Structure of the MRCQC-Chart

There is variety of literature available on developing variants of control charts for time between events situations. Based on the information presented in the previous section, we present the control structure of the suggested chart by utilizing the distribution function of the mixture distribution, i.e. $F(Q) = p_1 F_1(Q) + p_2 F_2(Q)$, $\sum_{i=1}^{2} p_i = 1$. Let $\psi_1 = \exp\left(-Q^2\lambda_1^2\right)$ the and $\psi_2 = \exp\left(-Q^2\lambda_2^2\right)$. We establish a logarithmic relationship between the densities of two nonconformities in order to obtain simplified expression for the control limits, i.e., $\psi_1 = (1 - \log(1-\tau))\exp\left(-Q^2\lambda_2^2\right)$, where τ is some specified constant i.e. $0 \leq \tau < 1$. This implies that: $F(Q) = p_1\left(1 - (1 - \log(1-\tau))\psi_2\right) + p_2(1 - \psi_2)$, after some simplification we obtained the following:

$$F(Q) = 1 - \psi_2\left(1 - p_1 \log(1-\tau)\right). \tag{14}$$

The selected value of missing information depends upon the fraction of nonconformities produced by each sub population. We construct a two-sided MRCQC-chart (by fixing the probability of false alarm rate α), and set $F(Q)$ in equation (13) equal to $(1-\alpha/2)$, $1/2$ and $\alpha/2$ for upper control limit (UCL), central line (CL) and lower control limit (LCL) respectively. Hence, the control structure of the suggested scheme is given by:

$$1 - \exp\left(-Q_U^2\lambda_2^2\right)\left[1 - p_1\log(1-\tau)\right] = 1 - \alpha/2, \qquad (i)$$
$$1 - \exp\left(-Q_C^2\lambda_2^2\right)\left[1 - p_1\log(1-\tau)\right] = 1/2, \qquad (ii)$$
$$1 - \exp\left(-Q_L^2\lambda_2^2\right)\left[1 - p_1\log(1-\tau)\right] = \alpha/2. \qquad (iii)$$

In order to find the expressions for UCL, CL and LCL, the previous expressions can be further reduced to the following forms:

$$\begin{aligned}
\text{UCL}: \ Q_U &= \frac{1}{\lambda_2}\left\{\ln\left(\frac{1-p_1\log(1-\tau)}{\alpha/2}\right)\right\}^{1/2}, \\
\text{CL}: Q_c &= \frac{1}{\lambda_2}\left\{\ln\left(\frac{1-p_1\log(1-\tau)}{1/2}\right)\right\}^{1/2}, \\
\text{LCL}: \ Q_L &= \frac{1}{\lambda_2}\left\{\ln\left(\frac{1-p_1\log(1-\tau)}{1-\alpha/2}\right)\right\}^{1/2}.
\end{aligned} \tag{15}$$

In the MRCQC-chart, Q (cumulative quantity between two nonconformities) is plotted on the chart against the corresponding sample numbers. When the cumulative quantity below the LCL sets off an alarm that the rate of occurrence of defects in the process may have shifted upward, that is, the process may have deteriorated, these unnatural variations should be explored in order to undertake a safety measure. If the plotted point above the UCL shifts downwards, the process may have improved. The lower and upper sided MRCQC-chart can be designed by equating $F(Q)$ in (13) by α and $(1-\alpha)$, respectively; obtaining the following: $Q_L = \frac{1}{\lambda_2}\left\{\ln\left(\frac{1-p_1\log(1-\tau)}{1-\alpha}\right)\right\}^{1/2}$ and $Q_U = \frac{1}{\lambda_2}\left\{\ln\left(\frac{1-p_1\log(1-\tau)}{\alpha}\right)\right\}^{1/2}$. Should be mentioned that, the value of λ_2 in a process is usually unknown; we can obtained an estimate by using the methodology discussed above in Section 2.

3.1. The SRCQC-Chart as a Special Case of the MRCQC -Chart

It is worth noting that the MRCQC-chart converges to the SRCQC-chart, which is established on a single component or simple Rayleigh distribution provided that $\tau = 0$. It is obvious that for $\tau = 0$, λ_1 (the rate of nonconformities from first sub population) λ_2 (the rate of nonconformities from second sub population) becomes equal, which leads to a simple Rayleigh distribution with a fraction of nonconformities $\lambda_1 = \lambda_2 = \lambda$. In a similar manner, $\tau = 0$ implies that $F(Q) = 1 - \psi_2$. Hence, it becomes a simple case of Rayleigh distribution, and the double control limits are designed as follows.

$$\begin{aligned}
\text{UCL}: Q_U &= \frac{1}{\lambda_2}\left\{\ln\left(\frac{\alpha}{2}\right)^{-1}\right\}^{1/2}, \\
\text{CL}: Q_c &= \frac{1}{\lambda_2}\left\{\ln\left(\frac{1}{2}\right)^{-1}\right\}^{1/2}, \\
\text{LCL}: Q_L &= \frac{1}{\lambda_2}\left\{\ln\left(1-\frac{\alpha}{2}\right)^{-1}\right\}^{1/2}.
\end{aligned} \tag{16}$$

If our concern is to determine the shift in the downfall or improvement direction, we only set a lower or upper limit for a one sided SRCQC-chart, e.g. $Q_L = \frac{1}{\lambda_2}\left[\ln(1-\alpha)^{-1}\right]^{1/2}$.

3.2. Estimation of Average Run Length

The run length of the control chart is defined as the sample number until a signal is delivered by the chart; the expectation of the run length is commonly known as average run length (ARL). The ARL is extensively used as a measure of performance in a control chart and it works as a random variable because of its probabilistic nature (cf. Quesenberry 2007 and Montgomery 2009). Ideally, the ARL should be large when the process is in control and small when the process is out of control. The algebraic expression for ALR_L, ARL_U and $\mathrm{ARL}_{L\&U}$ are obtained in simplified form (cf. Chan et al. 2002 and Majeed et al. 2012).

$$ARL_L = \frac{1}{1-(1-\alpha_L)^{\varphi}\left\{1-p_1\ln(1-\tau)\right\}^{1-\varphi}},$$

$$ARL_U = \frac{1}{(\alpha_U)^{\varphi}\left\{1-p_1\ln(1-\tau)\right\}^{1-\varphi}} \quad \text{and}$$

$$ARL_{L\&U} = \frac{1}{1-\left\{1-p_1\ln(1-\tau)\right\}^{1-\varphi}\left\{(1-\alpha_L)^{\varphi}-(\alpha_U)^{\varphi}\right\}}.$$

where $\varphi = \frac{\hat{\delta}}{\delta}$ and $\delta = \lambda_2^2$ is the magnitude of shift to be detected according to Chan et al. (2002, Proposition B of Appendix), and α_L and α_U are the probabilities of false alarms for LCL and UCL respectively. The performance measure ALR_L is used to examine the shift in deterioration, ALR_U is used to detect the shift in improvement, and performance measure $\mathrm{ARL}_{L\&U}$ is used to simultaneously determine the shift in downfall and progression. The computations of ARL are presented in pictorial form (cf. Figures 1-3) for different choices of false alarm rates as well as for different amounts of shift. Figures 1 $(a-d)$ represent the graphical display of ARL for the process progression, and show that the proposed control chart is not capable of early detection compared with a simple Rayleigh control chart. From this pictorial representation it can be see that the proposed scheme has an issue of non-maximal and upward biased ARL behavior for process progression. Figures 2 $(e-h)$ show a graphical representation of ARL for process downfall, and Figures 3 $(i-l)$ for process downfall and progression at the same time. From the later two pictorial descriptions, we conclude that the proposed control chart performs better in terms of early detection of shifts in downfall and downfall and progression simultaneously in comparison with simple Rayleigh control chart. It is also worth mentioning that the later two pictorial descriptions provide maximal and unbiased ARL behaviors for both progression and downfall.

3.3. Estimation of Average Length of Inspection

Average length of inspection (ALI) is another performance measure for control charts. The ALI required to observe a signal is $\frac{E(Q)}{\alpha} = E(Q) \times ARL$, Chan et al. (2002). The analogous ALIs for signal to appear on MRCQC-chart below the LCL, above the UCL, and either below the LCL or above the UCL, when the rate of occurrence of nonconformities in sample is λ_2 are as follows:

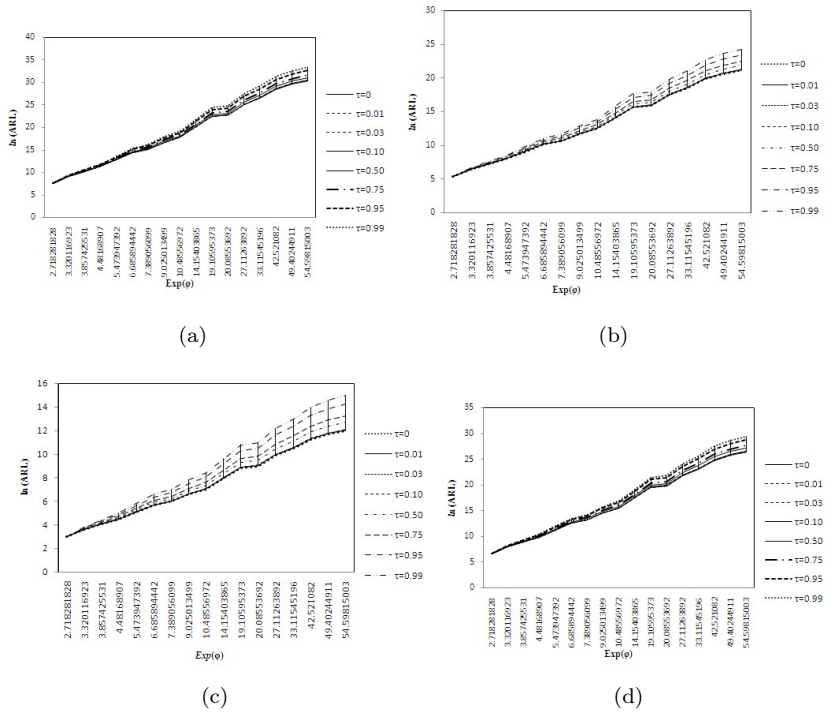

FIGURE 1: Average run length plot $\ln ARL_U$ against Exp (φ) for the MRCQC-chart to detect the shift in improvement when $a_U = 0.0005$, 0.005, 0.05, and 0.00135, respectively, with corresponding weight= 0.375.

$$ARI_L = \frac{1}{\hat{\lambda}_2}\frac{\sqrt{\pi}}{2}ARL_L,$$
$$\%ARI_U = \frac{1}{\hat{\lambda}_2}\frac{\sqrt{\pi}}{2}ARL_U \quad \text{and}$$
$$ARI_{L\&U} = \frac{1}{\hat{\lambda}_2}\frac{\sqrt{\pi}}{2}ARL_{L\&U}.$$

The simulation study shows that the Bayes estimates assuming informative (Nakagami) has a clear edge over square root gamma prior. This is because posterior risks are smaller under Nakagami prior. The ALIs are obtained using the Nakagami prior under two loss functions for the MRCQC-chart and the SRCQC-chart. They are represented graphically in Figures 4-6.

The comparisons are made using $\tau = 0.01$, $p_1 = 0.375$, $\varphi = 1.5$, $\alpha_L = \alpha_U = 0.0027$, 0.005 and 0.05 These results reveal that PLF is dominant for both MRCQC-charts and SRCQC-charts. Moreover, the MRCQC-chart outperforms the usual SRCQC-chart in the early detection of shifts.

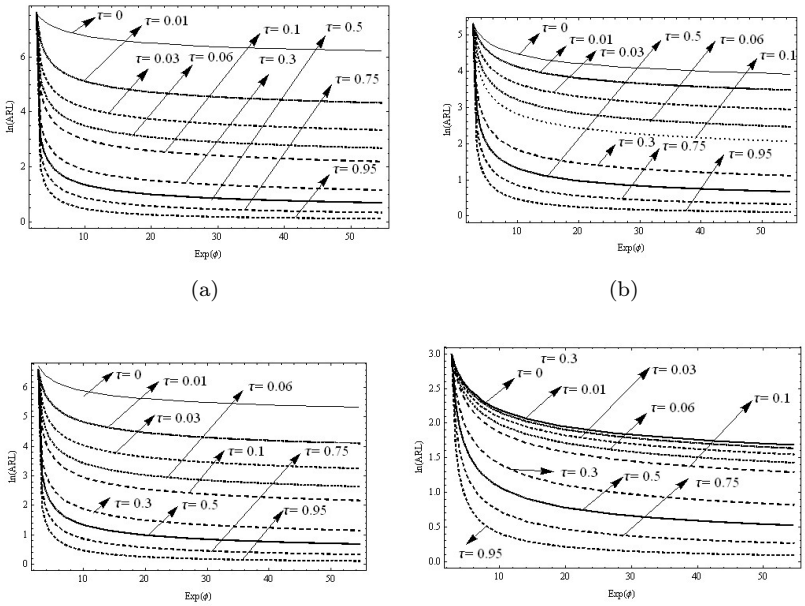

FIGURE 2: Average run length plot $\ln\text{ARL}_L$ against $\exp(\varphi)$ for MRCQC to identify the shift in deterioration under $\alpha_L = 0.0005$, 0.005, 0.05, and 0.00135, respectively, with corresponding weight= 0.375.

4. Illustrative Example (Compartive Study)

In this section, we analyze an example to illustrate the methodology discussed in the previous sections. In a high-quality process, defects occur at a rate of $\lambda_2 = 0.0002$ defect per unit quantity of produced products. The probability of false alarm is set at $\alpha = 0.0027$, and the mixing weights are set as $p_1 = 0.375$ and $p_2 = 0.625$. The value of the constant is $\tau = 0.01$. The lower and upper control limits and the central limit are calculated for the CQC, MCQC, SRCQC and MRCQC charts are as follows.

Double-limit CQC-Chart:

$$\textbf{UCL:}Q_U = \frac{-1}{0.0002}\ln\left(\frac{0.0027}{2}\right) = 33038.25$$

$$\textbf{LCL:}Q_L = \frac{-1}{0.0002}\ln\left(1-\frac{0.0027}{2}\right) = 6.76$$

$$\textbf{CL:}Q_C = \frac{-1}{0.0002}\ln\left(\frac{1}{2}\right) = 3465.74$$

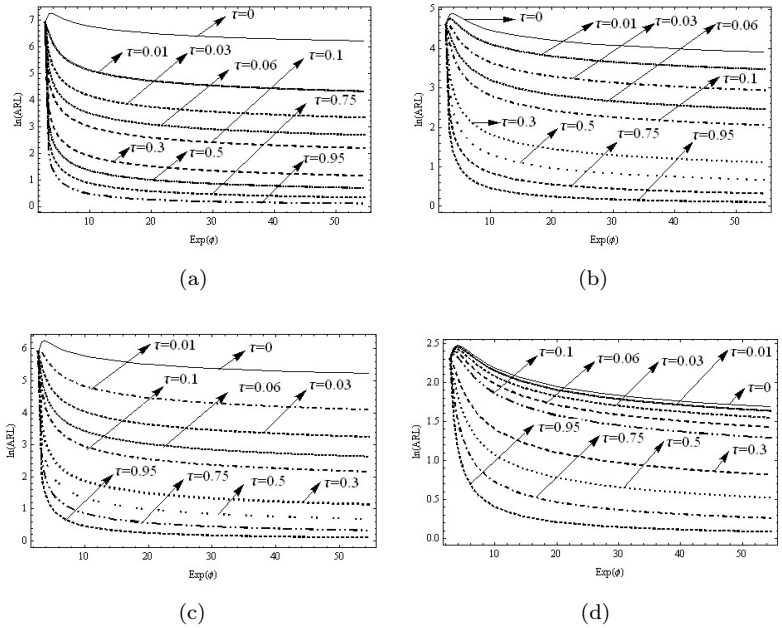

FIGURE 3: Average run length plot $\ln\text{ARL}_{L\&U}$ against $\exp(\varphi)$ for MRCQC to identify the shift in depreciation and development under $a_U = a_L = 0.0005$, 0.005, 0.05, and 0.00135, respectively, with corresponding weight $p_{1=}0.375$.

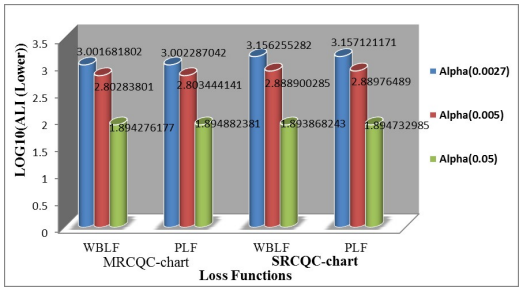

FIGURE 4: Average length of inspections (ALIs) displays for the MRCQC-chart to detect the shift in *downfall* $a_L = 0.0027$, 0.005, and 0.05, while $\tau = 0.01, p_1 = 0.375, \varphi = 1.5$.

Double-limit MCQC-Chart:

$$\textbf{UCL:}Q_U = \frac{-1}{0.0002}\ln\left(\frac{\frac{0.0027}{2}}{0.375\,(2-1)+1}\right) = 34630.52$$

$$\textbf{LCL:}Q_L = \frac{-1}{0.0002}\ln\left(\frac{1-\frac{0.0027}{2}}{0.375\,(2-1)+1}\right) = 1599.02$$

$$\textbf{CL:}Q_C = \frac{-1}{0.0002}\ln\left(\frac{\frac{1}{2}}{0.375\,(2-1)+1}\right) = 5058.00$$

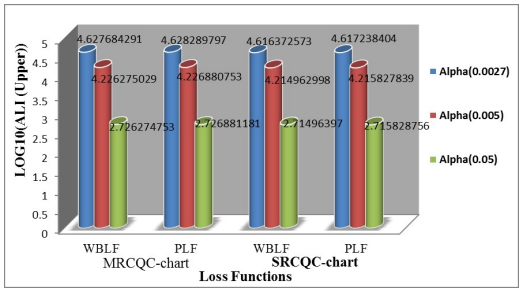

FIGURE 5: Average length of inspections (ALIs) displays for the MRCQC-chart to detect the shift in improvement $a_U = 0.0027$, 0.005 and 0.05 while $\tau = 0.01, p_1 = 0.375, \varphi = 1.5$.

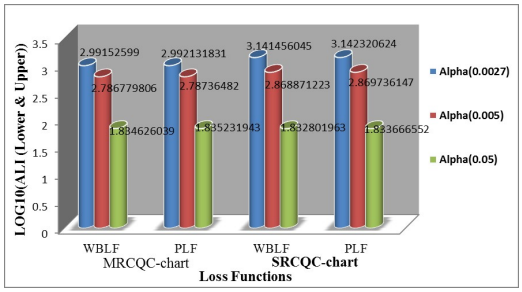

FIGURE 6: Average length of inspections (ALIs) displays for the MRCQC-chart to detect the shift in improvement $a_U = 0.0027$, 0.005 and 0.05 while $\tau = 0.01, p_1 = 0.375, \varphi = 1.5$.

Double-limit SRCQC-Chart:

$$\textbf{UC L:}Q_U = \frac{1}{0.0002}\left\{\ln\left(\frac{0.0027}{2}\right)^{-1}\right\}^{1/2} = 12852.7$$

$$\textbf{LCL:}Q_L = \frac{1}{0.0002}\left\{\ln\left(1-\frac{0.0027}{2}\right)^{-1}\right\}^{1/2} = 183.774$$

$$\textbf{CL:}Q_C = \frac{1}{0.0002}\left\{\ln\left(\frac{1}{2}\right)^{-1}\right\}^{1/2} = 4162.77.$$

Double-limit MRCQC-Chart:

$$\textbf{UCL:}Q_U = \frac{1}{0.0002}\left\{\ln\left(\frac{1-0.375\log\left(1-0.01\right)}{\frac{0.0027}{2}}\right)\right\}^{1/2} = 12856.3$$

$$\textbf{LCL:}Q_L = \frac{1}{0.0002}\left\{\ln\left(\frac{1-p_1\log\left(1-0.01\right)}{1-\frac{0.0027}{2}}\right)\right\}^{1/2} = 357.516$$

$$\textbf{CL:}Q_C = \frac{1}{0.0002}\left\{\ln\left(\frac{1-0.375\log\left(1-0.01\right)}{\frac{1}{2}}\right)\right\}^{1/2} = 4174.05$$

The raw data from the process are codified in Table 3. The size of each sample is 400 units. In Table 3, the number 199.4 in sample 5 is the remainder of the sample after the defect is observed. The same is true for the number 154.0 in sample 56. In this Table, 'i.c.', 'n.d.', 'o.c.' and 'im.' mean 'in control', 'no decision', 'out of control' and 'has been improved', respectively. A double-limit CQC, MCQC, SRCQC-chart and MRCQC-chart is provided in Figure 7.

Table 3: Inspection results for raw data from a process.

Sample number	Defect Observed?	Cumulative Value of Q since last reset	Signal?	Reset Q to zero?
1	No	$400 \geq LCL$	i.c	No
2	No	$800 \geq LCL$	i.c	No
3	No	$1200 \geq LCL$	i.c	No
4	No	$1600 \geq LCL$	i.c	No
5	Yes	$1800.6 \geq LCL$	i.c	Yes
5	No	199.4^*	n.d.	No
6	Yes	$250 < LCL$	o.c.	Yes
1	No	$400 \geq LCL$	i.c	No
2	No	800	i.c	No
:		:	:	:
:		:	:	:
32	No	12800	i.c	No
33	No	$13200 > UCL$	im	No
34	No	13600	im	No
55	No	22000	im	No
56	Yes	$22246 > UCL$	im	Yes
56	No	154^*	n.d.	No
57	No	$554 \geq LCL$	i.c	No
58	No	954	i.c	:
59	No	1354	i.c	:
:	:	:	:	:
:	:	:	:	:
77	No	8554	i.c	No
78	Yes	$8773.4 \geq LCL$	i.c	Yes
:	:	:	:	:
:	:	:	:	:

From Table 3, it is noted that an asterisk "*" appears when a non-conformity has been observed and process is resetting and quantity with an asterisk "*" sign is added to next sample quantity when process is resetting in improved region. It is also noted that "▲" sign seems in the pictorial description (given in Figure 7) of the hypothetical data set with the quantity having an asterisk "*" sign and whenever a defect is observed and cumulative quantity at that time above the LCL. It is also worth mentioning that whenever a defect is observed and cumulative quantity is, at that time, below the LCL, then the whole process is restarted and "+" shows a pictorial description of the tabular data set when observed cumulative quantity above the UCL. Figure 7 shows the charting structure of the CQC, MCQC, SR-CQC and MRCQC charts in light of aforementioned data set where specific lines represent the control structure of the CQC, MCQC, SRCQC and MRCQC charts,

respectively. In the MCQC-chart, the "▲" at sample 6 is clearly shown to be the above the ln(LCL-MCQC), which does not indicate the process is out of control. In terms of corresponding CQC, SRCQC and MRCQC charts, however, this point is below the LCL, which indicates the process is out of control. According to the MCQC-chart, this appears above the LCL unjustly, which signifies an in control situation, when the process is really out of control. Thus MRCQC-chart outperforms in the deterioration region in comparison with its competitors, i.e. the CQC, SRCQC and MCQC charts. At this stage Q is reset to zero and a new quantity is considered for analysis. On both charts the sign "⧫" for sample number 32 is very close to UCL, which makes it much harder to see that it is above the UCL of both the SRCQC amd MRCQC charts. When an inspection of sample numbers 33 and 34 has been completed, the cumulative quantity of items inspected are 13200 and 3600 > UCL of SRCQC and MRCQC charts. Also, the "+" is an indication that the process may have improved.If however ln(cumulative quantity) is below the UCL of CQC and MCQC charts the process has no improvement. According to the MRCQC-chart, the sign "*" for the remainders of the sample numbers 5 and 56 show doubtful state, whereas the RCQC-chart gives the wrong signal of an in control situation at sample number 5. On MRCQC-chart, the sign "+" appears beyond the UCL, which is an indication that the process may have improved and hence MRCQC perform better in comparison to its competitor(s).

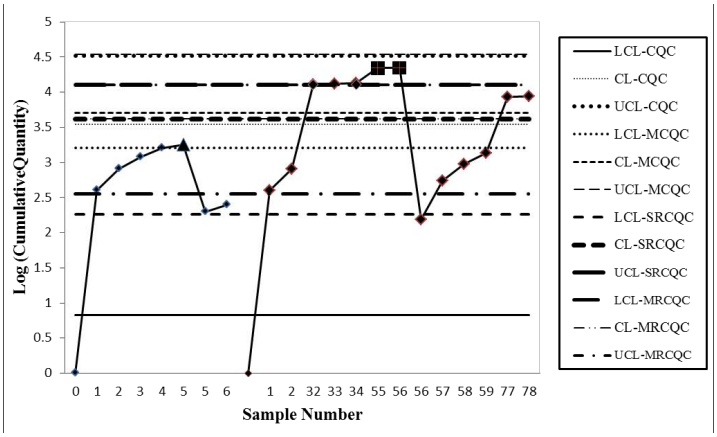

FIGURE 7: Comparison of MRCQC and SRCQC with existing CQC and MCQC control charts.

5. Concluding Remarks

This study has investigated Bayesian estimation for the mixture Rayleigh model and proposed its application in process monitoring. A new MRCQC chart was developed for industrial applications and a SRCQC chart is discussed as a special case for single component distribution. We have examined the performance of the proposal for different rates of defective units. It was observed that the MRCQC chart is quite efficient at early detection of shifts. In some situations, the

single component SRCQC-chart may not perform well and the mixture MRCQC-chart serves is more effective in terms of early shift detection in deterioration and improvement regions. Moreover, a Bayesian technique enhanced the performance of estimates of mixture models in terms of being precise.

This scope of this study may be extended to other lifetime distributions such as Gumbel, Power, Lognormal and Gamma models. Memory structures such as cumulative sum (CUSUM) and exponentially weighted moving average (EWMA) control charts may also be developed along these lines. Furthermore, multivariate generalization of MRCQC-charts may be an interesting topic for additional research in this sector.

[Received: November 2014 — Accepted: July 2015]

References

Aslam, M. (2003), 'An application of prior predictive distribution to elicit the prior density', *Journal of Statistical Theory and Applications* **2**(1), 70–83.

Banjevic, D., Jardine, A. K. S., Makis, V. & Ennis, M. (2001), 'A control-limit policy and software for condition-based maintenance', *INFOR* **39**, 32–50.

Calvin, T. (1983), 'Quality control techniques for zero defects', *IEEE Transactions on Components Hybrids and Manufacturing Technology* **6**(3), 323–328.

Chan, L. Y., Lin, D. K. J., Xie, M. & Goh, T. N. (2002), 'Cumulative probability control charts for geometric and exponential process characteristics', *International Journal of Production Research* **40**(1), 133–150.

Chan, L. Y., Xie, M. & Goh, T. N. (2000), 'Cumulative quantity control charts for monitoring production processes', *International Journal of Production Research* **38**(2), 397–408.

Degroot, M. H. (1970), *Optimal statistical decision*, McGraw-Hill Inc.

Grimshaw, S. D., Collings, B. J., Larsen, W. A. & Hurt, C. R. (2001), 'Eliciting factor importance in a designed experiment', *Technometrics* **43**(2), 133–146.

Jenkinson, D. J. (2005), The elicitation of probabilities a review of the statistical literature, Beep working paper, University of Sheffield, United Kingdom.

Leon, J. C., Vazquez-Polo, J. F. & Gonzalez, L. (2003), 'Environmental and resource economics', *Kluwer Academic Publishers* **26**, 199–210.

Majeed, M. Y., Aslam, M. & Riaz, M. (2012), 'Mixture cumulative count control chart for mixture geometric process characteristics', *Quality & Quantity* **26**, 1–19.

Mendenhall, W. & Hadar, R. J. (1958), 'Estimation of parameters of mixed exponentially distributed failure time distribution from censored life test data', *Biometrika* **45**(3-4), 504–520.

Montgomery, D. C. (2009), *Introduction to Statistical Quality Control*, 6 edn, John Wiley & Sons, New York.

Norstrom, J. G. (1996), 'The use of precautionary loss functions in risk analysis', *IEEE Transactions on Reliability* **45**(3), 400–403.

O'Hagan, A., Buck, C. E., Daneshkhah, A., Eiser, J. E., Garthwaite, P. H., Jenkinson, D. J., Oakley, J. E. & Rakow, T. (2006), *Uncertain Judgements: Eliciting expert probabilities*, John Wiley & Sons, New York.

Quesenberry, C. P. (2007), *SPC Methods for Quality Improvement*, John Wiley & Sons, Toronto.

Sun, F. B., Yang, J., del Rosario, R. & Murphy, R. (2001), A conditional-reliability control-chart for the post-production extended reliability-test, *in* 'Proceedings Annual Reliability and Maintainability Symposium', pp. 64–9.

Xie, M. & Goh, T. N. (1992), 'Some procedures for decision making in controlling high yield processes', *Quality and Reliability Engineering International* **8**(4), 355–360.

Xie, M., Goh, T. N. & Kuralmani, V. (2000), 'On optimal setting of control limits for geometric chart', *International Journal of Reliability Quality and Safety Engineering* **7**(1), 17–25.

Xie, M., Goh, T. N. & Ranjan, P. (2002), 'Some effective control chart procedures for reliability monitoring', *Reliability Engineering and System Safety* **19**(77), 143–150.

Xie, M., Goh, T. N. & Tang, X. Y. (2000), 'Data transformation for geometrically distributed quality characteristics', *Quality and Reliability Engineering International* **16**(1), 9–15.

Appendix

$$\hat{\lambda}_{1(WBLF)} = \frac{\sum_{k=0}^{n-r}\binom{n-r}{k} Beta\left(n-r_2-k+c_1, r_2+k+d_1\right) \frac{\Gamma(r_1+a_1+1)\Gamma(r_2+a_2)}{\left\{a_1/b_1+\xi_{1j}\left(q_{1j}\right)\right\}^{(r_1+a_1+1)}\left\{a_2/b_2+\xi_{2j}\left(q_{2j}\right)\right\}^{(r_2+a_2)}}}{\sum_{k=0}^{n-r}\binom{n-r}{k} Beta\left(n-r_2-k+c_1, r_2+k+d_1\right) \frac{\Gamma(r_1+a_1+1/2)\Gamma(r_2+a_2)}{\left\{a_1/b_1+\xi_{1j}\left(q_{1j}\right)\right\}^{(r_1+a_1+1/2)}\left\{a_2/b_2+\xi_{2j}\left(q_{2j}\right)\right\}^{(r_2+a_2)}}},$$

$$\rho\left(\hat{\lambda}\right)_{1(WBLF)} = 1 - \frac{\left(\sum_{k=0}^{n-r}\binom{n-r}{k} Beta\left(n-r_2-k+c_1, r_2+k+d_1\right) \frac{\Gamma(r_1+a_1+1/2)\Gamma(r_2+a_2)}{\left\{a_1/b_1+\xi_{1j}\left(q_{1j}\right)\right\}^{(r_1+a_1+1/2)}\left\{a_2/b_2+\xi_{2j}\left(q_{2j}\right)\right\}^{(r_2+a_2)}}\right)^2}{\Omega\sum_{k=0}^{n-r}\binom{n-r}{k} Beta\left(n-r_2-k+c_1, r_2+k+d_1\right) \frac{\Gamma(r_1+a_1+1)\Gamma(r_2+a_2)}{\left\{a_1/b_1+\xi_{1j}\left(q_{1j}\right)\right\}^{(r_1+a_1+1)}\left\{a_2/b_2+\xi_{2j}\left(q_{2j}\right)\right\}^{(r_2+a_2)}}}.$$

$$\hat{\lambda}_{2(WBLF)} = \frac{\sum_{k=0}^{n-r}\binom{n-r}{k} Beta\left(n-r_2-k+c_1, r_2+k+d_1\right) \frac{\Gamma(r_1+a_1)\Gamma(r_2+a_2+1)}{\left\{a_1/b_1+\xi_{1j}\left(q_{1j}\right)\right\}^{(r_1+a_1)}\left\{a_2/b_2+\xi_{2j}\left(q_{2j}\right)\right\}^{(r_2+a_2+1)}}}{\sum_{k=0}^{n-r}\binom{n-r}{k} Beta\left(n-r_2-k+c_1, r_2+k+d_1\right) \frac{\Gamma(r_1+a_1)\Gamma(r_2+a_2+1/2)}{\left\{a_1/b_1+\xi_{1j}\left(q_{1j}\right)\right\}^{(r_1+a_1)}\left\{a_2/b_2+\xi_{2j}\left(q_{2j}\right)\right\}^{(r_2+a_2+1/2)}}},$$

$$\rho\left(\hat{\lambda}\right)_{2(WBLF)} = 1- \frac{\left(\sum_{k=0}^{n-r}\binom{n-r}{k} Beta\left(n-r_2-k+c_1, r_2+k+d_1\right) \frac{\Gamma(r_1+a_1)\Gamma\left(r_2+a_{2+1/2}\right)}{\left\{a_1/b_1+\xi_{1j}\left(q_{1j}\right)\right\}^{(r_1+a_1)}\left\{a_2/b_2+\xi_{2j}\left(q_{2j}\right)\right\}^{(r_2+a_2+1/2)}}\right)^2}{\Omega\sum_{k=0}^{n-r}\binom{n-r}{k} Beta\left(n-r_2-k+c_1, r_2+k+d_1\right) \frac{\Gamma(r_1+a_1)\Gamma(r_2+a_2+1)}{\left\{a_1/b_1+\xi_{1j}\left(q_{1j}\right)\right\}^{(r_1+a_1)}\left\{a_2/b_2+\xi_{2j}\left(q_{2j}\right)\right\}^{(r_2+a_2+1)}}}.$$

$$\hat{p}_{1(WBLF)} = \frac{\sum_{k=0}^{n-r}\binom{n-r}{k} Beta\left(n-r_2-k+c_1+2, r_2+k+d_1\right) \frac{\Gamma(r_i+a_i)}{\left\{a_i/b_i+\xi_{ij}(q_{ij})\right\}^{(r_i+a_i)}}}{\sum_{k=0}^{n-r}\binom{n-r}{k} Beta\left(n-r_2-k+c_1+1, r_2+k+d_1\right) \frac{\Gamma(r_i+a_i)}{\left\{a_i/b_i+\xi_{ij}(q_{ij})\right\}^{(r_i+a_i)}}},$$

$$\rho\left(\hat{p}_1\right)_{(WBLF)} = 1- \frac{\left(\sum_{k=0}^{n-r}\binom{n-r}{k} Beta\left(n-r_2-k+c_1+1, r_2+k+d_1\right) \frac{\Gamma(r_i+a_i)}{\left\{a_i/b_i+\xi_{ij}(q_{ij})\right\}^{(r_i+a_i)}}\right)^2}{\Omega\sum_{k=0}^{n-r}\binom{n-r}{k} Beta\left(n-r_2-k+c_1+2, r_2+k+d_1\right) \frac{\Gamma(r_i+a_i)}{\left\{a_i/b_i+\xi_{ij}(q_{ij})\right\}^{(r_i+a_i)}}}.$$

Where Ω is formulized as:

$$\Omega = \sum_{k=0}^{n-r}\binom{n-r}{k} Beta\left(n-r_2-k+c_1, r_2+k+d_1\right) \frac{\Gamma\left(r_i+a_i\right)}{4\left\{a_i/b_i+\xi_{ij}\left(q_{ij}\right)\right\}^{(r_i+a_i)}}$$

$$\hat{\lambda}_{WBLF} = \frac{\Gamma\left(c_3+n+1\right)}{\Gamma\left(c_3+n+1/2\right)\sqrt{\sum_{i=1}^{n} q_i^2+c_3/d_3}},$$

$$\rho\left(\hat{\lambda}_{WBLF}\right) = 1 - \left(\frac{\Gamma\left(c_3+n\right)}{2\left(\sum_{i=1}^{n} q_i^2+c_3/d_3\right)^{c_3+n}}\right)^{-1} \times \left(\frac{\Gamma\left(c_3+n+1/2\right)}{\left(\sum_{i=1}^{n} q_i^2+c_3/d_3\right)^{c_3+n+1/2}}\right)^2 \times \left(\frac{\Gamma\left(c_3+n+1\right)}{\left(\sum_{i=1}^{n} q_i^2+c_3/d_3\right)^{c_3+n+1}}\right)^{-1}.$$

$$\hat{\lambda}_{PLF} = \sqrt{\frac{(c_3+n)}{(\sum_{i=1}^{n} q_i^2 + c_3/d_3)}},$$

$$\rho\left(\hat{\lambda}_{PLF}\right) = 2\left(\sqrt{\frac{(c_3+n)}{(\sum_{i=1}^{n} q_i^2 + c_3/d_3)}} - \frac{\Gamma\left(c_3+n+1/2\right)}{\Gamma\left(c_3+n\right)\left(\sum_{i=1}^{n} q_i^2 + c_3/d_3\right)^{1/2}}\right).$$